Supporting Materials for

Electrical Modulation of High-Q Guided-Mode Resonances Using Graphene

Seyoon Kim[1,†,*], Ju Young Kim[2,†], Min Seok Jang[2,*], and Victor W. Brar[1,*]

[1]Department of Physics, University of Wisconsin-Madison, Madison, Wisconsin 53706, United States

[2]School of Electrical Engineering, Korea Advanced Institute of Science and Technology, Daejeon 34141, Republic of Korea

[*]skim886@wisc.edu

[*]jang.minseok@kaist.ac.kr

[*]vbrar@wisc.edu

[†]These authors contributed equally to this work.

Contents

Supporting Note S1: Fano formula

Optical resonance can be described by the Fano resonance formalism when it arise from the interaction between a discrete eigenstate (an indirect coupling pathway) and a continuum (a direct coupling pathway) [1]. In the proposed structure, the guided-mode resonance and the Fabry-Perot resonance correspond to the discrete eigenstate and the continuum, respectively. Therefore, the line shapes of the resonances can be modeled by the Fano formula [1,2]:

$$I_{\mathrm{Fano}}(\omega) = \frac{I_{\mathrm{res}}}{1+q^2}\frac{(q+\Omega^2)}{1+\Omega^2} + I_{\mathrm{non-res}} \qquad \text{(S1)}$$

where ω is the light frequency, q is the Fano parameter determining the asymmetric profile, I_{res} and $I_{\mathrm{non\text{-}res}}$ describe the resonant peak amplitude and the non-resonant contribution, respectively. Ω is the dimensionless frequency defined by $\Omega=(\omega-\omega_{\mathrm{res}})/\gamma$, where ω_{res} is the resonant frequency and γ corresponds to the damping rate of the resonance. Here, the damping rate (γ) is the summation of the absorption rate (γ_a) and the scattering rate (γ_s). The damping rate can be evaluated by $\gamma=\Delta\omega/2$, where $\Delta\omega$ is the full-width half maximum of the resonance. From these parameters, the Q-factor is determined by $\omega_{\mathrm{res}}/\Delta\omega$.

To analyze the resonances presented in the manuscript, we fit the spectra into the Fano formula. As an example, the fitting results of the Fig. 2(c-d) in the manuscript are shown in Fig. S1. The solid lines are the spectra obtained in full-wave simulations, and the dashed lines illustrate the Fano profiles fitted by Eq. (S1).

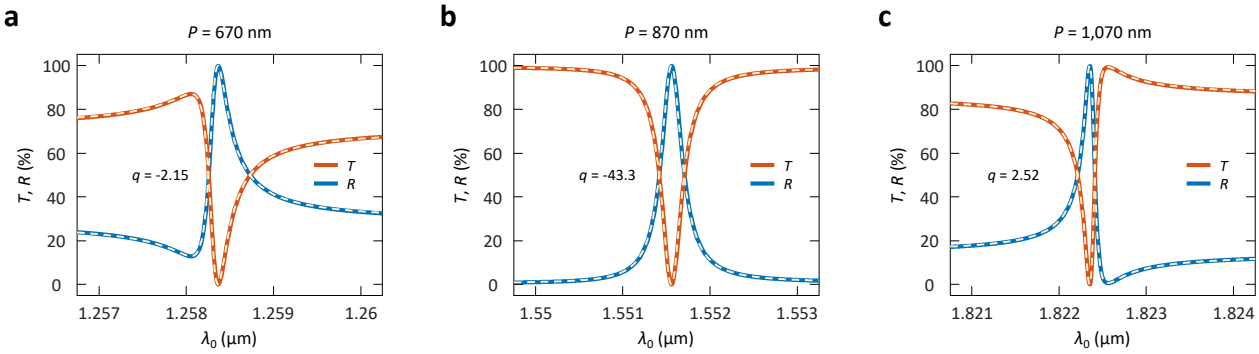

Figure S1. (**a**-**c**) Transmission (T) and reflection (R) spectra presented in Fig. 2(a) in the manuscript (solid lines) and Fano profiles (dashed lines) fitted by Eq. (S1) with different Fano parameters (q).

As shown in Fig. S1, the Fano parameters (q) determine the asymmetric profile. When $|q|\sim1$, the interaction between the guided-mode resonance and the Fabry-Perot resonance is balanced, and it produces the general asymmetric form of the Fano resonances, as shown in Figs. S1(a) and (c). The sign of the Fano parameter characterizes the phase relation between the two resonances, and it regulates the direction of the Fano profile. On the other hand, the guided-mode resonance, or the discrete eigenstate, dominates the Fano response if $|q|\gg1$. In this case, the Fano response in Eq. (S1) becomes the Lorentzian function. In this case, the overall high-Q resonant feature is invoked by the guided-mode resonance dominantly, and the Fabry-Perot resonance determines the non-

resonant term [1]. As a result, both the transmission and the reflection transit rapidly between zero and unity at the resonance, as illustrated in Fig. S1(b).

Supporting Note S2: Effect of intrinsic absorption in dielectric materials

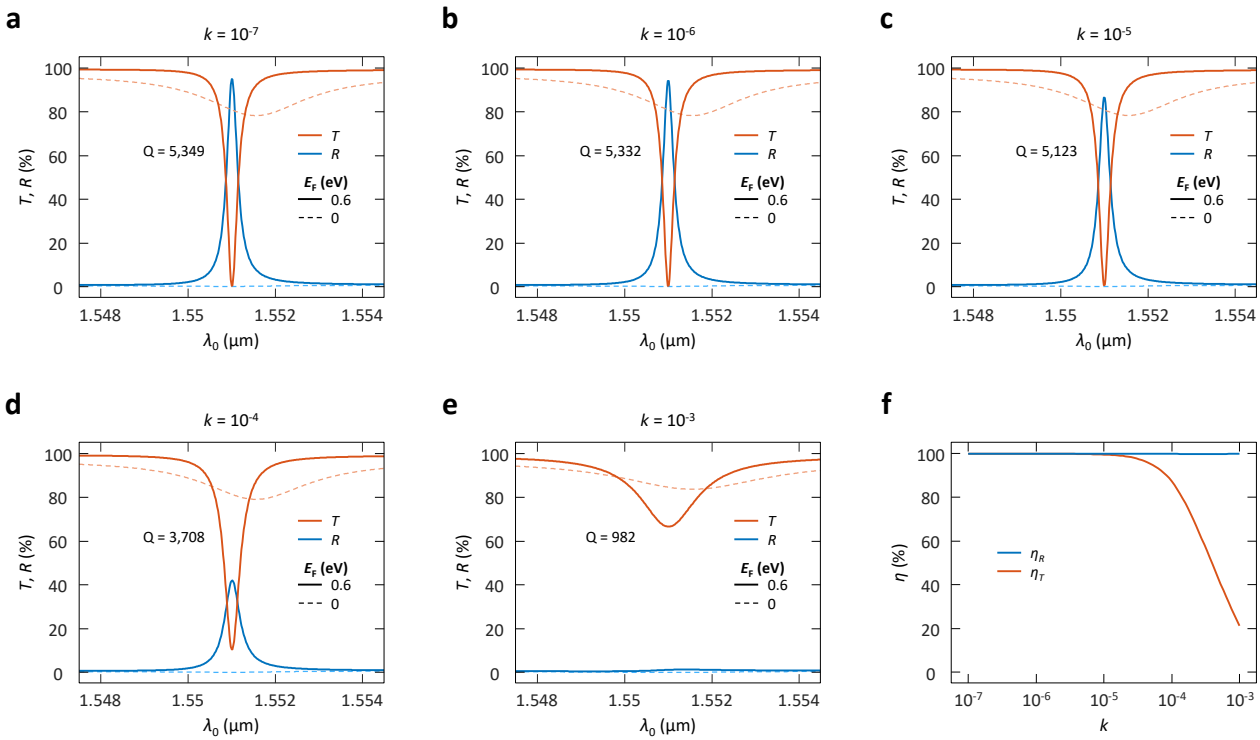

Figure S2. (**a**-**e**) Transmission (T) and reflection (R) spectra with different k values, or the imaginary parts of the refractive indices, imposed on SiO_2, SiN_x, and Si. The structural parameters are equal to those in Fig. 3 in the manuscript. (**f**) Transmission efficiency ($\eta_T = 1\text{-}T_{min}/T_{max}$), reflection efficiency ($\eta_R = 1\text{-}R_{min}/R_{max}$) at E_F=0.6 eV as a function of the k value.

Supporting Note S3: Temporal coupled mode theory

The temporal coupled mode theory (TCMT) is a formalism that couples localized resonant modes within resonant structures to incoming and outgoing radiation modes in different radiation ports [3-5]. The theory is able to provide a scattering matrix for various photonic platforms hosting resonances, and is especially useful for dealing with high-Q resonances.

Based on the TCMT, the dynamic amplitude (a) for a single resonance can be described by

$$\frac{da}{dt} = (-i\omega_{\text{res}} - \gamma_{\text{s}} - \gamma_{\text{a}})a + \boldsymbol{\kappa}^T \mathbf{s}^+ \qquad \text{(S2)}$$

$$\mathbf{s}^- = \mathbf{C}\mathbf{s}^+ + a\mathbf{d} \tag{S3}$$

where $\mathbf{s}^+$ and $\mathbf{s}^-$ are the incoming wave and the outgoing wave, respectively, $\boldsymbol{\kappa}$ is the coupling coefficients between the resonance and the incoming wave, $\mathbf{d}$ is the resonance-assisted coupling coefficient, and $\mathbf{C}$ describes the direct couplings between the incoming wave and the outgoing wave.

As described in Supporting Note S1, the guided-mode resonance, or the indirect coupling pathway, dominates the high-Q resonance. In addition, the contribution of the the Fabry-Perot resonances on the overall resonance, or the direct coupling pathway, is negligible because $T_{\text{non-res}}$ and $R_{\text{non-res}}$ are almost unity and zero, respectively, when the guided-mode resonance is not present. In this case, we can assume that the diagonal elements (C_{11} and C_{22}) of the $\mathbf{C}$ are zero. Considering the energy conservation and the reciprocity ($\mathbf{d}^\dagger\mathbf{d}=2\gamma_s$, $\boldsymbol{\kappa}=\mathbf{d}$, and $\mathbf{C}\mathbf{d}^*=-\mathbf{d}$), we can obtain the coefficients as

$$\boldsymbol{\kappa} = \mathbf{d} = \begin{pmatrix} \sqrt{\gamma_s} e^{i\theta_1} \\ \sqrt{\gamma_s} e^{i\theta_2} \end{pmatrix} \tag{S4}$$

$$\mathbf{C} = \begin{pmatrix} 0 & -e^{i(\theta_1+\theta_2)} \\ -e^{i(\theta_1+\theta_2)} & 0 \end{pmatrix} \tag{S5}$$

where θ_1 and θ_2 corresponds to the phase of the coupling coefficients. Here, we obtain $|\kappa_i| = |d_i| = \sqrt{\gamma_s}$ with an assumption of slowly varying perturbation on each port [3]. In addition, the s_2^- is zero because there is no incident light from the back side. Using these parameters, the reflectance (R), the transmittance (T), and the absorption (A) are derived as Eqs. (S6-S8) at a steady state ($da/dt=-i\omega a$).

$$R_{\text{TCMT}}(\omega) = \left|\frac{s_1^-}{s_1^+}\right|^2 = \frac{\gamma_s^2}{(\omega-\omega_{\text{res}})^2+\gamma^2} \tag{S6}$$

$$T_{\text{TCMT}}(\omega) = \left|\frac{s_2^-}{s_1^+}\right|^2 = \frac{\gamma_s^2 - 2\gamma_s\gamma}{(\omega-\omega_{\text{res}})^2+\gamma^2} + 1 \tag{S7}$$

$$A_{\text{TCMT}}(\omega) = 1 - R_{\text{TCMT}}(\omega) - T_{\text{TCMT}}(\omega) = \frac{2\gamma_s\gamma - 2\gamma_s^2}{(\omega-\omega_{\text{res}})^2+\gamma^2} \tag{S8}$$

When we compare these equations with the Fano formula in Eq. (S1), we can notice an important point of similarity. As described in Supporting Note S1, the resonant spectra are fitted with $|q|\gg1$ because the guided-mode resonances dominate the systems. In this case, Eq. (S1) becomes a Lorentzian form as

$$I_{\text{Fano}}(\omega) \approx \frac{I_{\text{res}}\gamma^2}{(\omega-\omega_{\text{res}})^2+\gamma^2} + I_{\text{non-res}} \tag{S9}$$

where $R_{\text{non-res}}\approx0$, $T_{\text{non-res}}\approx1$, and $A_{\text{non-res}}\approx0$. In an ideal case, we can calculate the γ_s/γ analytically from the γ and the I_{res} given from the Fano formula fitting.

In the evaluation of the γ_s/γ, one issue is that the non-resonant amplitudes ($I_{\text{non-res}}$) slightly differ from the ideal values. Indeed, this deviation comes from the non-resonant absorption in graphene and the non-infinite Fano parameter (q), which results in non-zero, albeit very small, diagonal elements in the direct scattering matrix in Eq.

(S5). To compensate for this deviation, we replace the offsets of Eqs. (S6-S8) with the $I_{\text{non-res}}$ evaluated in the Fano formula, as given in Eqs. (S10-S12). Then, we can obtain the γ_s/γ that match the R, T, and A spectra with minimal errors. These approximations are valid because the Fano fitting results still satisfy the conditions of $R_{\text{non-res}}\approx 0$, $T_{\text{non-res}}\approx 1$, $A_{\text{non-res}}\approx 0$, and $|q|\gg 1$.

$$R_{\text{TCMT}}(\omega) \approx \frac{\gamma_s^2}{(\omega-\omega_{\text{res}})^2+\gamma^2} + R_{\text{non-res}} \tag{S10}$$

$$T_{\text{TCMT}}(\omega) \approx \frac{\gamma_s^2 - 2\gamma_s\gamma}{(\omega-\omega_{\text{res}})^2+\gamma^2} + T_{\text{non-res}} \tag{S11}$$

$$A_{\text{TCMT}}(\omega) \approx \frac{2\gamma_s\gamma - 2\gamma_s^2}{(\omega-\omega_{\text{res}})^2+\gamma^2} + A_{\text{non-res}} \tag{S12}$$

The calculated γ_s/γ are presented in Fig. S3(a) as a function of the graphene Fermi level, and the γ_a/γ is given by 1-γ_s/γ. Figures S3(b-d) show the gate-dependent A, T, and R maps evaluated by Eqs. (S10-S12), and they show good agreement with the full-wave simulation results presented in Figs. 3(b-d) in the manuscript. It indicates the TCMT properly extracts the gate-dependent γ_s/γ.

In addition to the calculation of the scattering rate and the absorption rate, the TCMT analysis shows the critical coupling of the high-Q resonance. From Eqs. (S8) or (S12), we can see that the $A_{\text{TCMT}}(\omega=\omega_{\text{res}})$ is maximized when $\gamma_s/\gamma=1/2$, or $\gamma_a=\gamma_s$. This condition corresponds to critical coupling, where the overall absorption is maximized as the absorption loss and the scattering loss are balanced [3,6].

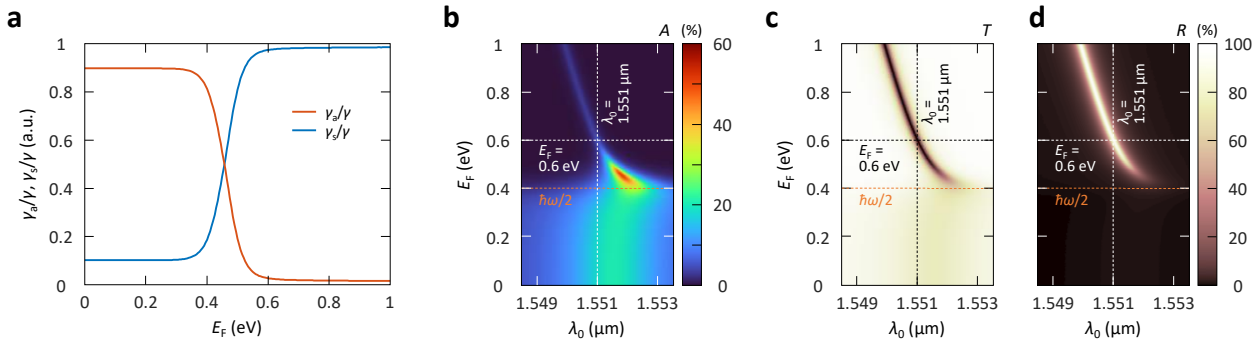

Figure S3. (**a**) Gate-dependent absorption rate ratio (γ_a/γ) and scattering rate ratio (γ_s/γ) calculated from the TCMT. (**b**) Gate-dependent absorption (A), (**c**) transmittance (T), and (**d**) reflectance (R) maps calculated from the TCMT as a function of λ_0.

Supporting References

[1] M. F. Limonov, M. V. Rybin, A. N. Poddubny, Y. S. Kivshar. *Nat. Photonics* **2017**, *11*, 543.

[2] K. Koshelev, S. Lepeshov, M. K. Liu, A. Bogdanov, Y. Kivshar. *Phys. Rev. Lett.* **2018**, *121*, 193903.

[3] H. A. Haus. *Waves and fields in optoelectronics*. (Prentice-Hall, **1984**).

[4] S. Fan, W. Suh, J. D. Joannopoulos. *J. Opt. Soc. Am. A* **2003**, *20*, 569.

[5] W. Suh, Z. Wang, S. H. Fan. *IEEE J. Quantum Electron.* **2004**, *40*, 1511.

[6] J. P. Wu, H. L. Wang, L. Y. Jiang, J. Guo, X. Y. Dai, Y. J. Xiang *et al. J. Appl. Phys.* **2016**, *119*, 203107.